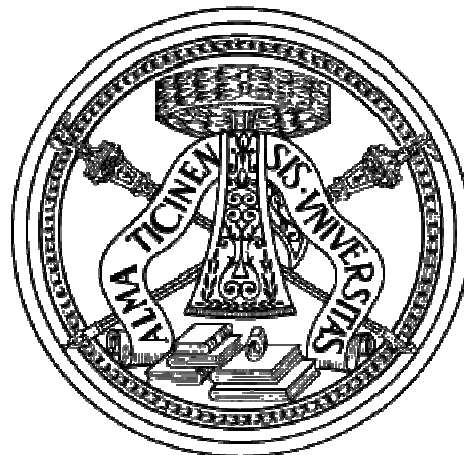




***Raffaele Ponzini***

# **Applicazioni del calcolo scientifico all'ambito biomedicale**





## *Order of the presentation*

- Biomed project at CILEA
- Computer aided engineering in biomed application
- Computational haemodynamics: a tasking environment
- CFD applications
- Application of CFD algorithms to human flow data



- ❑ Feb. 2004: start of my PhD program at the Bioengineering Dept. of the Politecnico di Milano (Advisor: A. Redaelli)
- ❑ 2005: Scientific Collaboration with MOX (C. Vergara; A. Veneziani)
- ❑ 2005: Scientific Collaboration with Politecnico di Torino (U. Morbiducci)
- ❑ 2006: Scientific Collaboration with G. Rizzo (IBFN-CNR)
- ❑ 2009: Written agreement with IBFN-CNR for study bio-image processing and HPC environment



# Computer aided engineering workflow

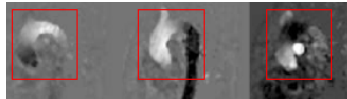
PRE-PROCESSING

COMPUTATION

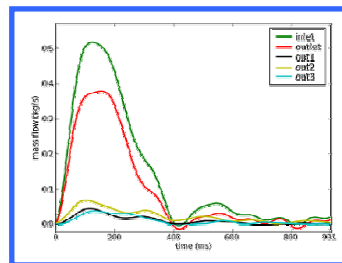
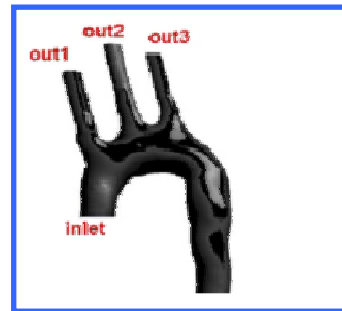
POST  
PROCESSING

COMPUTATIONAL

PHYSICAL

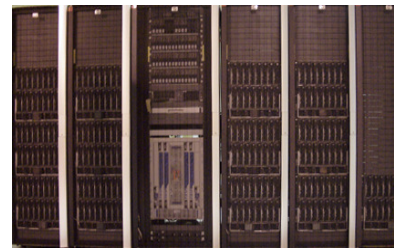


MODEL



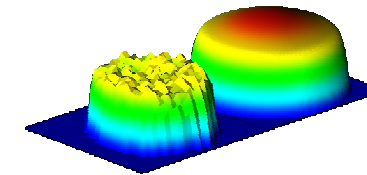
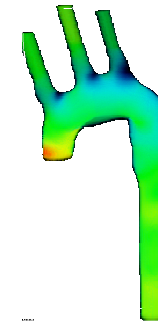
MODEL

SOLVING



HPC ENVIRONMENT

VISUALIZATION

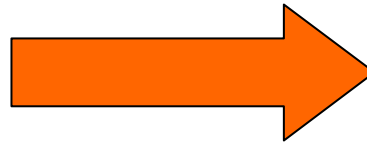


RESULTS



## *physical model*

- In vitro
- Animal models



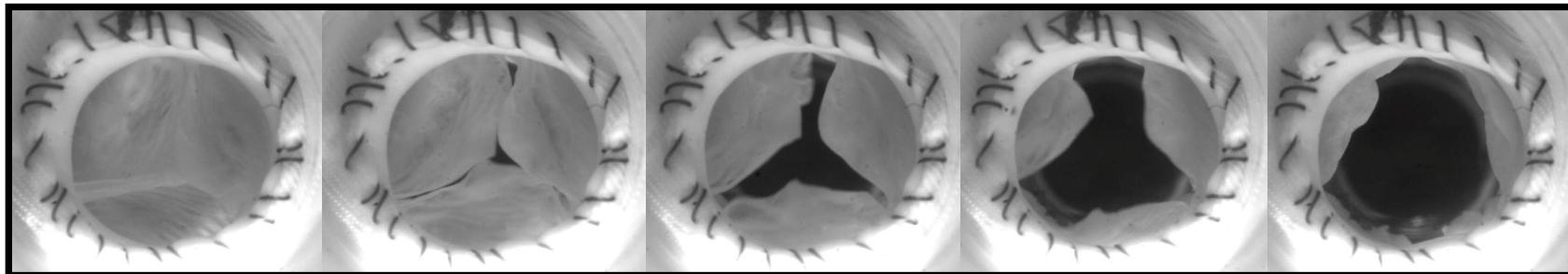
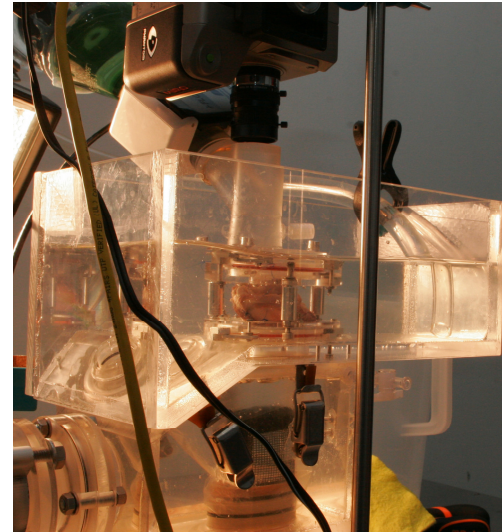
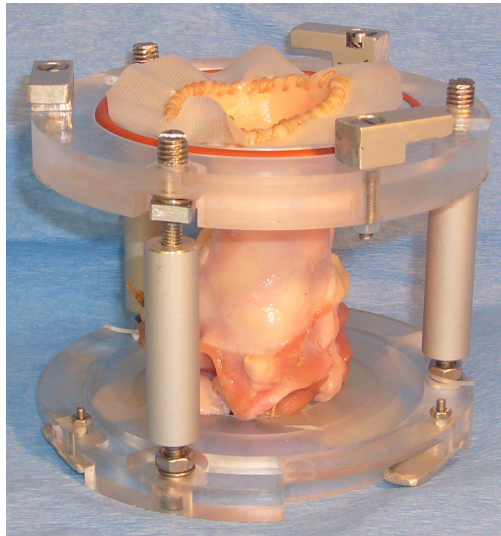
**Measures**

**Measures are necessary to built**  
**reliable CAE models**



## *in vitro models*

<http://www.forcardiolab.it/>



**0 ms**

**19.26 ms**

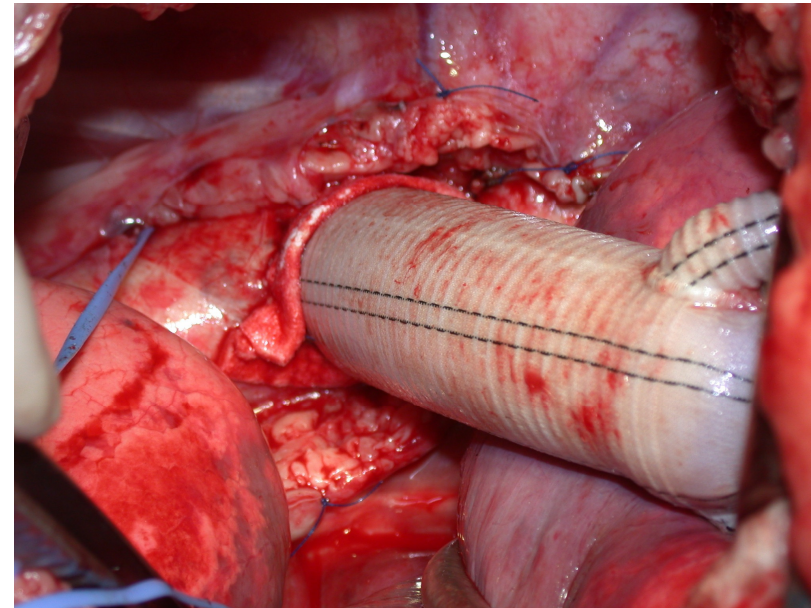
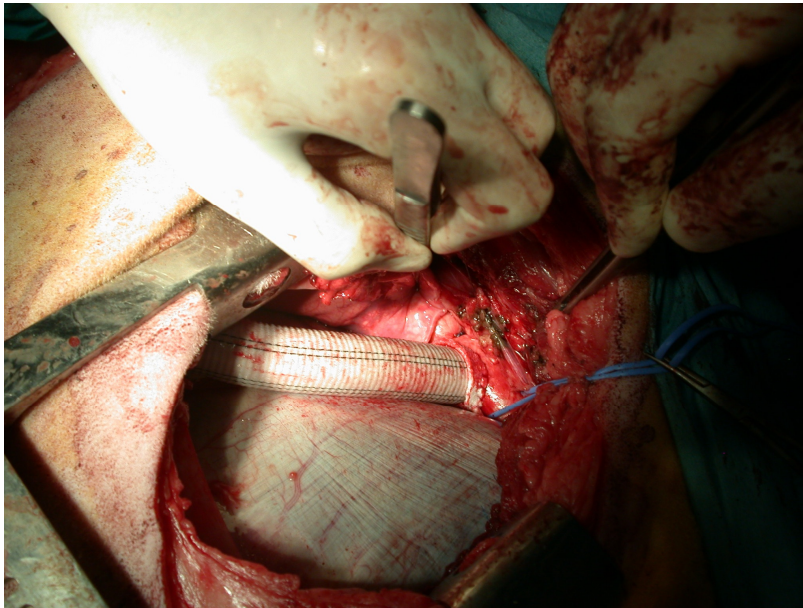
**24.88 ms**

**28.09 ms**

**33.71 ms**



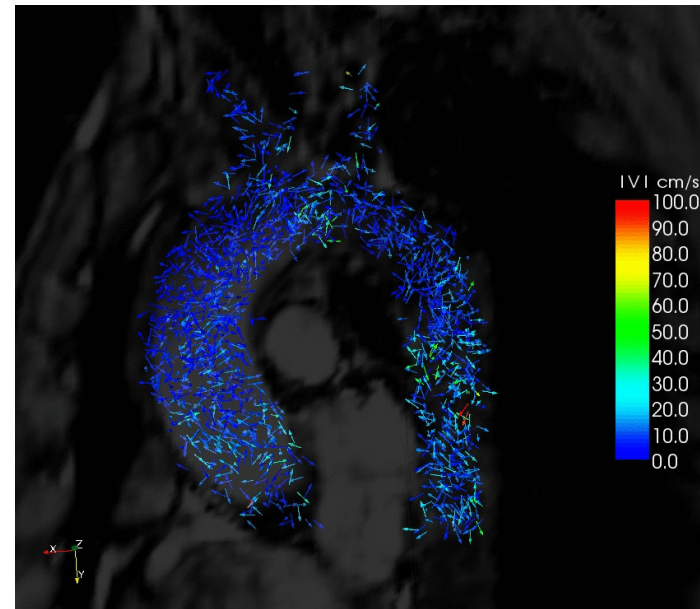
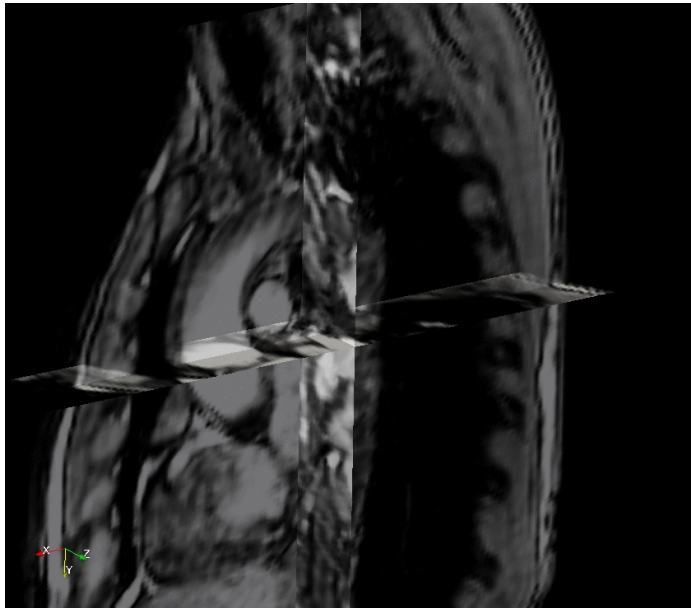
## *animal models*



Impianto protesico aortico in politetrafluoroetilene (PTFE) in una pecora  
eseguita da Fabio Acocella e Stefano Brizzola  
del Dipartimento Di Scienze Cliniche Veterinarie  
Facolta' Di Medicina Veterinaria  
Universita' Degli Studi Di Milano



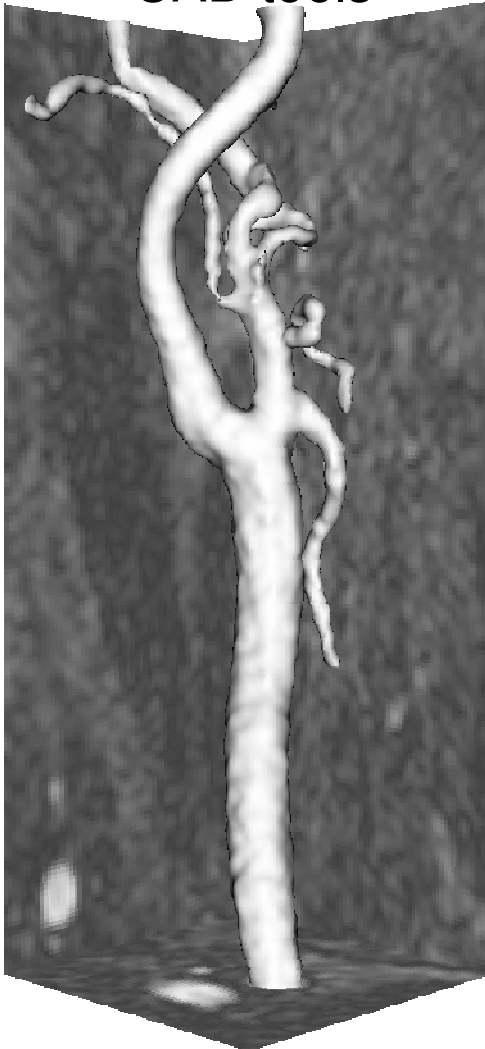
## *In vivo image based data*





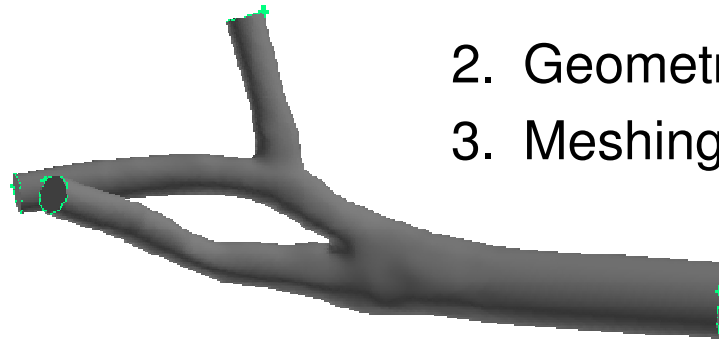
## *computational model*

1. Image processing or CAD tools

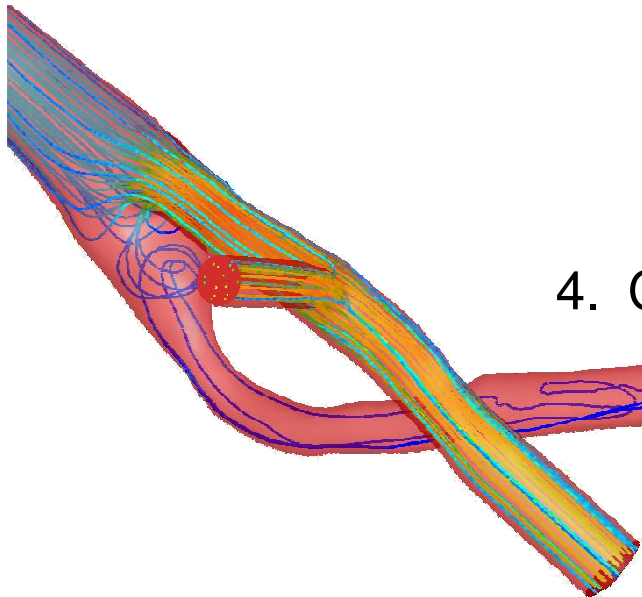


2. Geometry modeler

3. Meshing tools



4. CFD/Structural solvers





## *computational model*

- System of PDE (Navier-Stokes equations) defined in 3D domain
- + Initial Conditions
- + Boundary Conditions
- + Rheological properties of the fluid (blood)

Open Source  
Academic  
In house

Commercial

Finite  
Volumes

Finite  
Elements

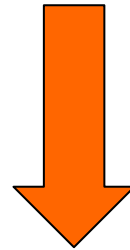
Lattice  
Boltzmann

Spectral  
methods



## *computational model*

**(Exact) Analytical solution is not available:  
Numerical (Approximated) solution of the problem**

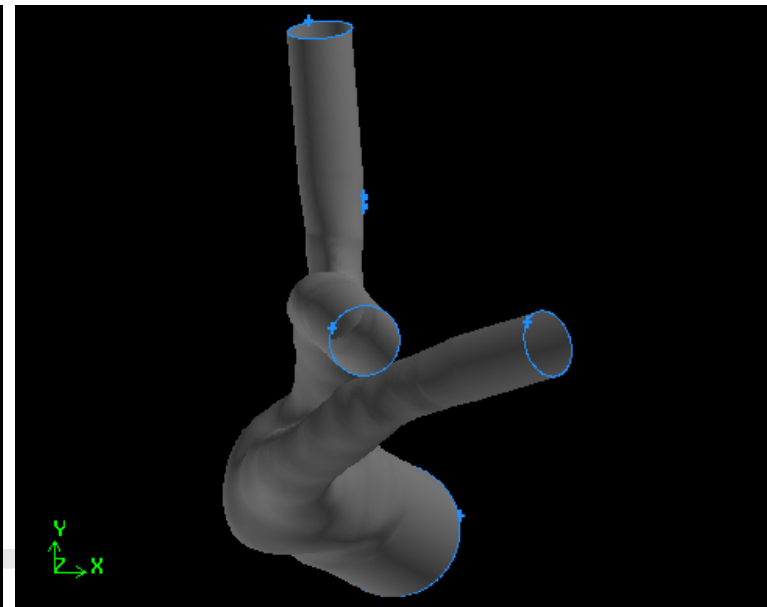
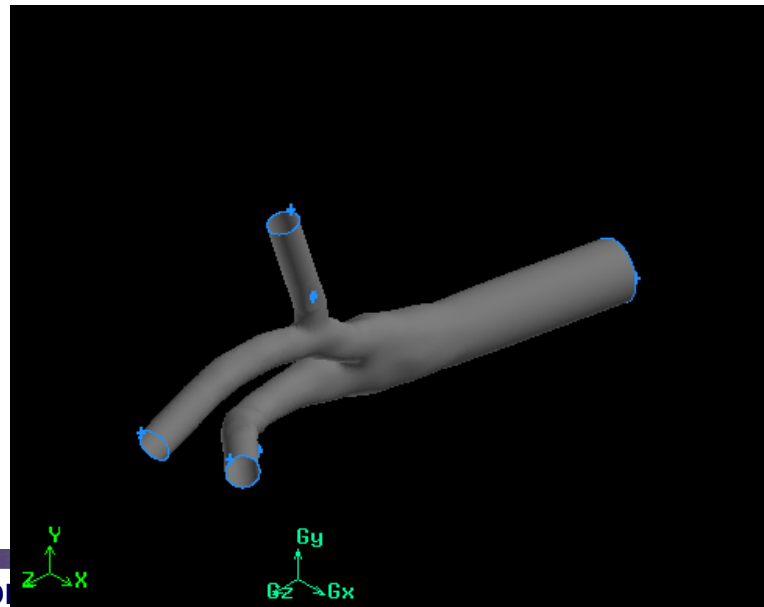
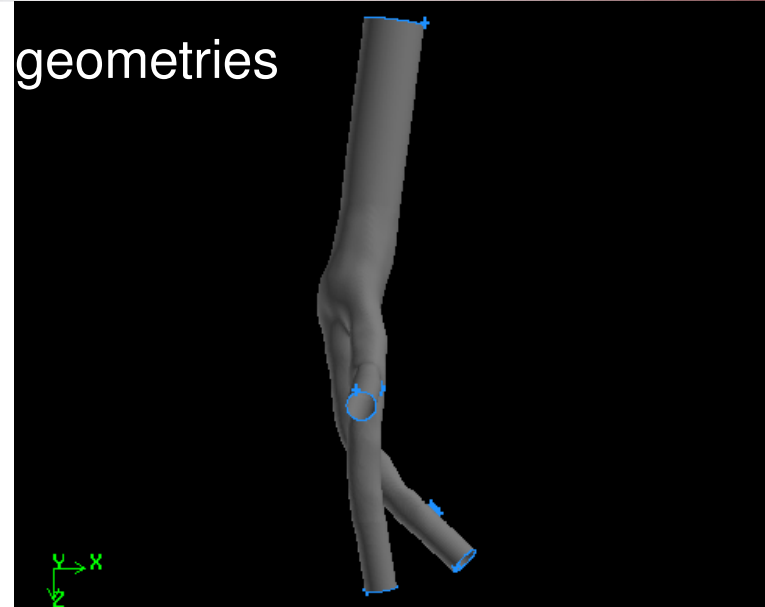
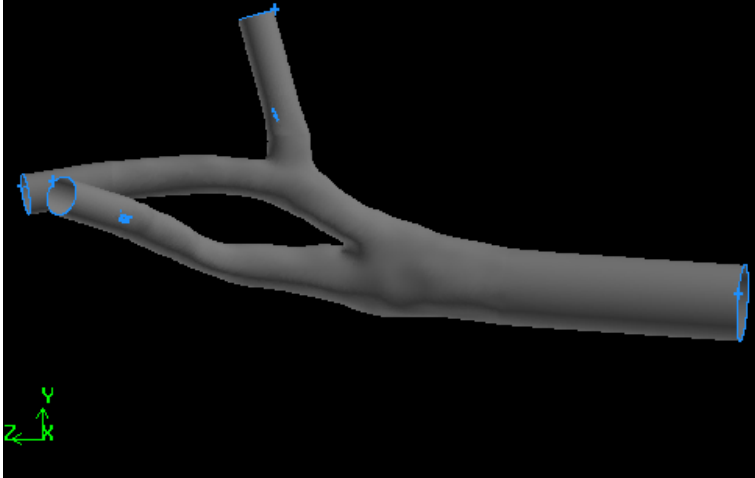


a tasking environment



## A tasking environment: Geometry

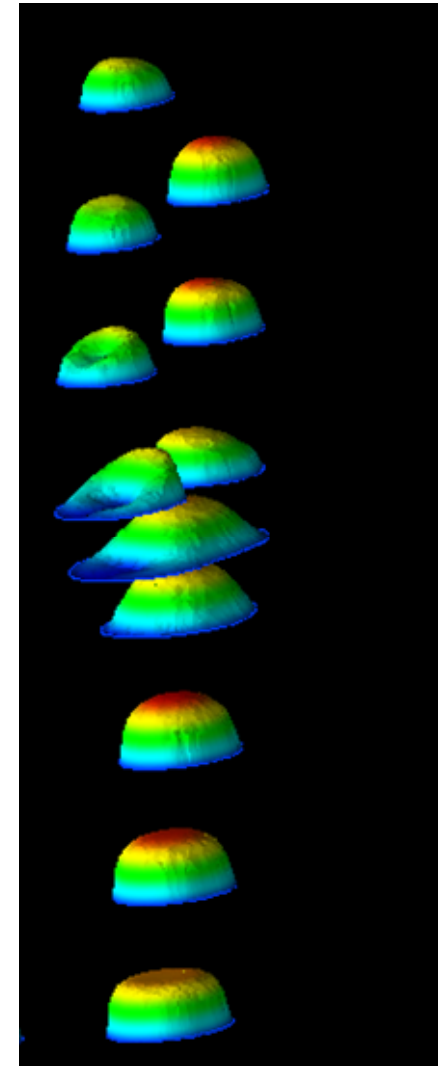
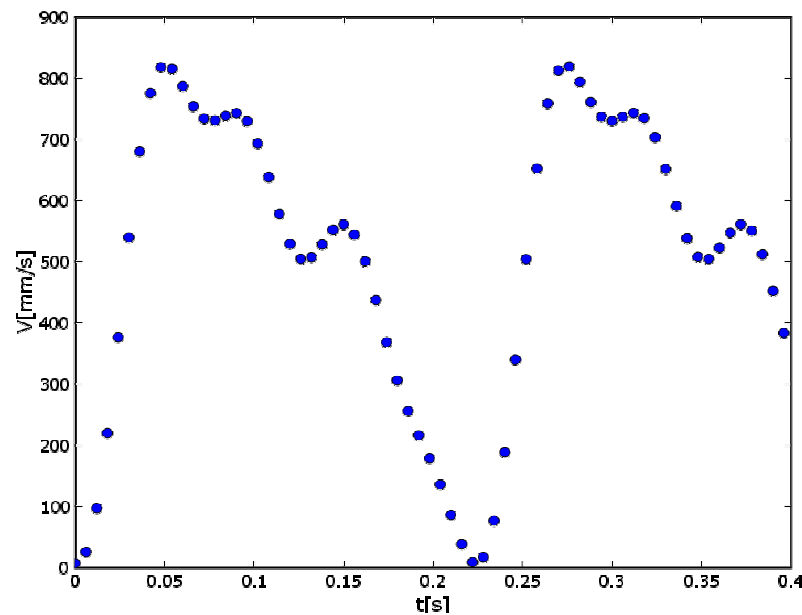
□ fully 3D complex geometries





## *A tasking environment: Boundary conditions*

- time dependent flow waveforms
- Spatial/temporal dependent velocity profiles
- Spatial/temporal dependent wall deformation

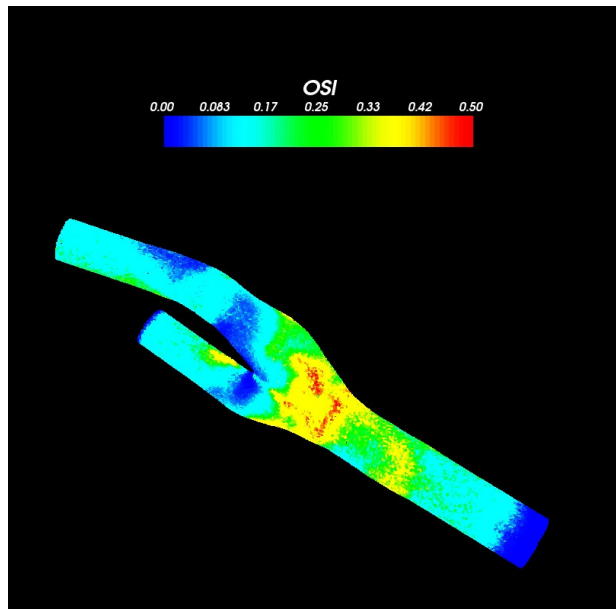




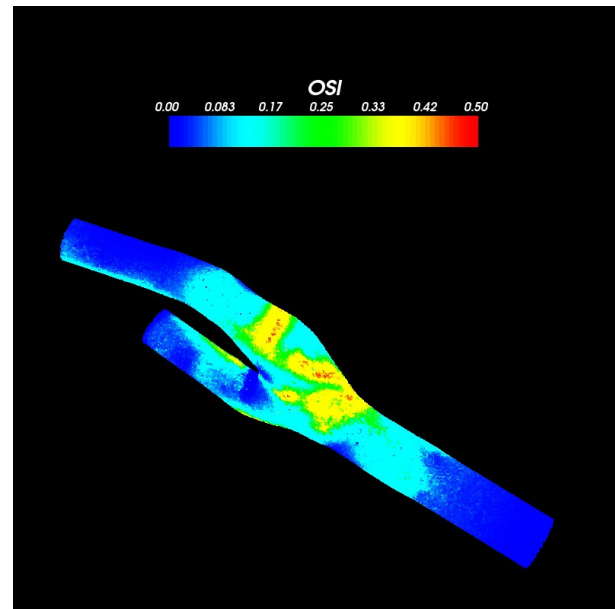
## *A tasking environment: rehology*

□ non-Newtonian fluid properties:

Carreau model



Newton model





## *A tasking environment: knowledge*

- limited 'experimental' knowledge on:
  - Wall-properties (Young's modulus?)
  - Fluid-to-wall interaction (wall displacements?)
  - Spatial/temporal velocity profiles distribution (accuracy of the measures in space&time?)
  - ...

.... but there's a GOOD news:

**Reynolds** numbers are very low compared to other engineering applications (below 2000)



## *Solving environment*



Lagrange.cilea.it

2928 cores Intel Xeon quad-cores

36 TFlops peak performance

IB DDR 2.0 Gb/s



## ***Reliable CFD-based Doppler flow rate estimates***

Doppler technique is the most used non invasive method to estimate in vivo the flow rate.

- Standard Doppler technique records the maximum velocity value in a point (centerline value) along time
- Usual blood volume Doppler estimates are performed using the maximum velocity value and an a-priori hypothesis on the shape of the spatial velocity profile across the vessel section:

-1- cylindrical symmetry

-2- parabola/flat:  $K_A=0.5/1.0$

$$Q_A = k_A \times V_M \times A$$

- The parabolic profile hypothesis has been successfully tested for time averaged flow rate estimation in coronary vessels (Doucette 1992 Circulation)

However, from theory (Womersley, 1955 J. Physiol), clinical observation (Jenny 2000 Ultr Med Biol) and computational models (Perktold 1998 J Biomech) the hypothesis of a parabolic profile seems untrue



## ***Reliable CFD-based Doppler flow rate estimates***

In 2006, **we designed a novel fully CFD-based protocol** (Ponzini, 2006 Ultrasound Med Biol) to simulate blood flow dynamics and Doppler procedure which:

- uses the CFD to achieve data
- performs CFD simulation without the imposition of the spatial velocity profiles (Veneziani and Vergara, 2005 Int J Num Meth Fluids);
- fitting parameters
- validate results



Such approach provides a **more general formula (with the respect to the a-priori)** based on a dimensionless parameters (**Womersley number based**):

$$Q_W = k_W \times V_M \times A$$



## ***Objective***

Up to now:

**the reliability of the new Womersley-based** approach has been validated in silico (i.e. using CFD) (Ponzini, 2006 Ultrasound Med Biol; Ponzini, 2008 Med. Eng. Phys.) :

-1- on idealized geometries (rigid/deformable walls)

-2- on realistic geometries:

carotid artery bifurcations (rigid walls),

Y-shaped bypass grafts (rigid walls),

TCPC (rigid walls)

**the sensitivity analysis** (to HR, Radius, Vmax) of the new Womersley-based approach has been performed using variational analysis method (Vergara, 2009 Comp. Meth. and Prog. in Biomed.) and

**the straightforward applicability** of the method to a non ad-hoc velocimetry clinical dataset has been shown (Vergara, 2009)

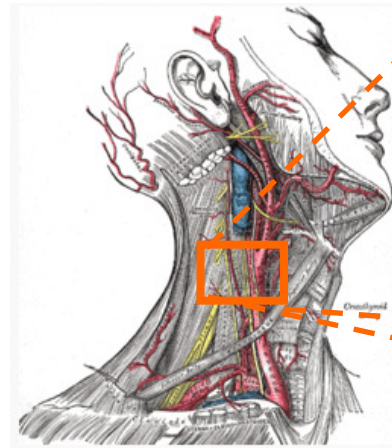
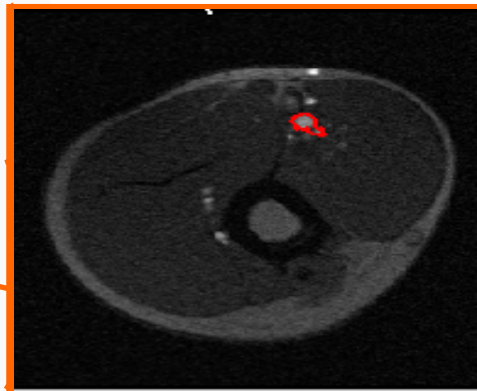
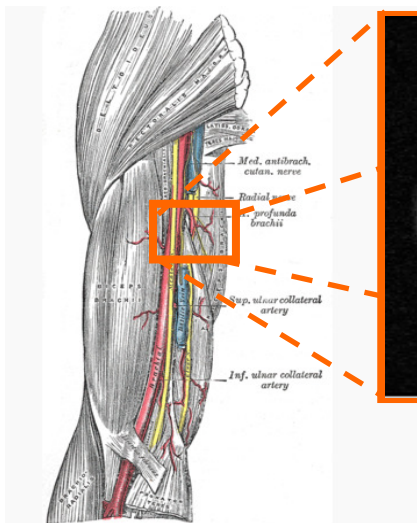
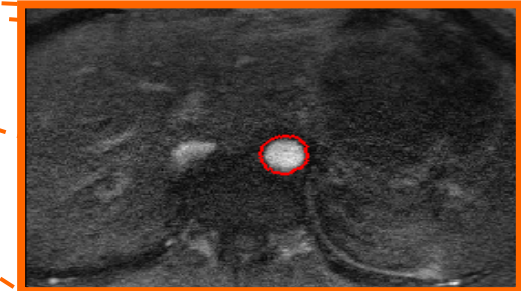
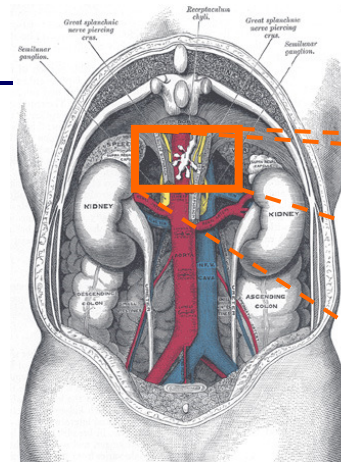
**Here an ad hoc in vivo validation using 2D Phase Contrast MRI is presented**



## Protocol set-up: 30 points dataset

### 30 points dataset:

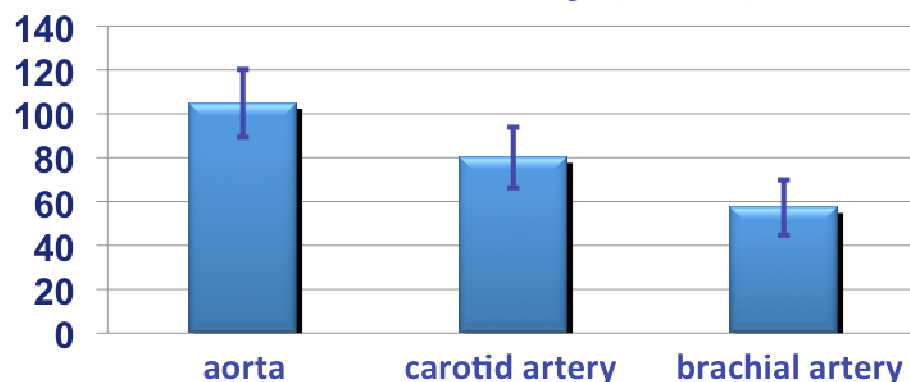
- 10 healthy volunteers age (age 23-48, all males)
- 3 arterial sites (small/medium/large)
- baseline-condition
- no branching/bending/tapered regions (**cylindrical symmetry HP**)



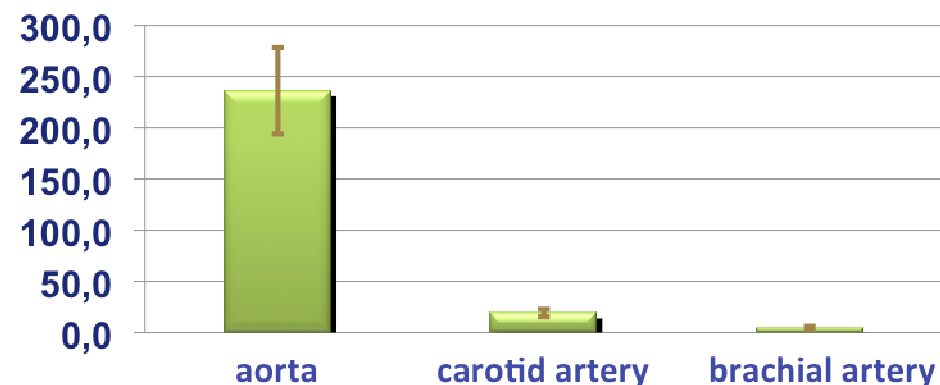


## *In-vivo data*

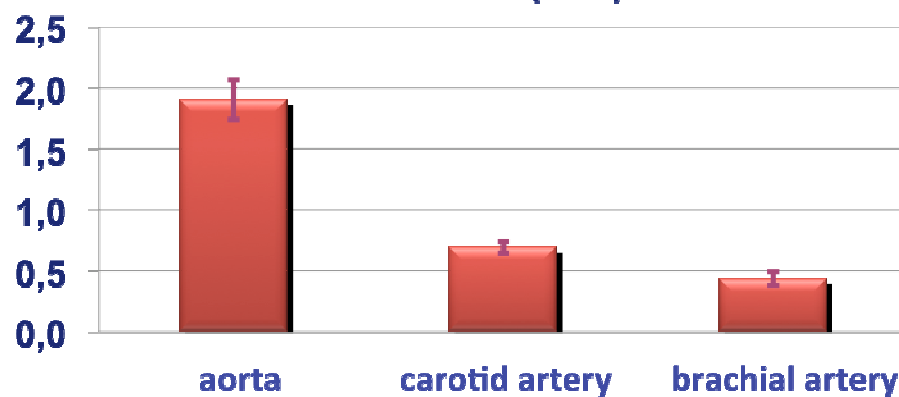
### Maximum Velocity (cm s<sup>-1</sup>)



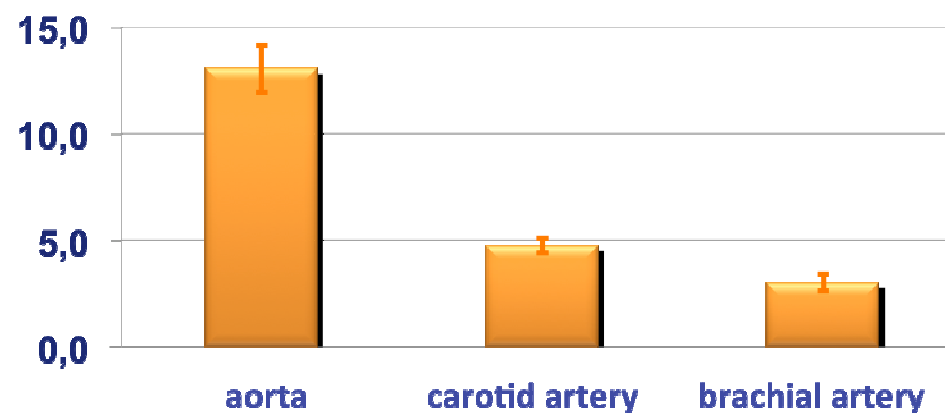
### Flow rate (cm<sup>3</sup> s<sup>-1</sup>)



### Diameter (cm)



### Womersley number





# In-vivo data processing: a 'Doppler-like' acquisition

## Cine PCMRI dataset

frame-0

frame-1

frame-2

frame-3

**frame-4**

frame-5

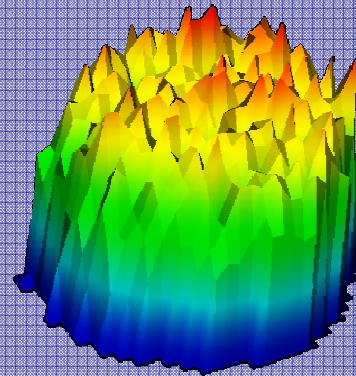
frame-6

frame-7

frame-8



## Full PCMRI dataset



## Flow rate computation (Gold Standard)

$$Q_{GS} \equiv \sum_{pi} V_{pi} \times A_{pi}$$

- *Radius*
- *Maximum velocity*
- *Heart-rate*

$$Q_E = k \times V_M \times \sum_{pi} A_{pi}$$

$k = k_A$  (a-priori)

$k = k_W$  (Womersely number-based)

**Doppler-like parameters**

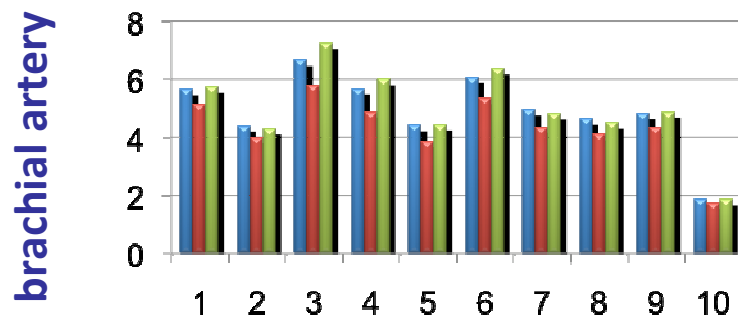
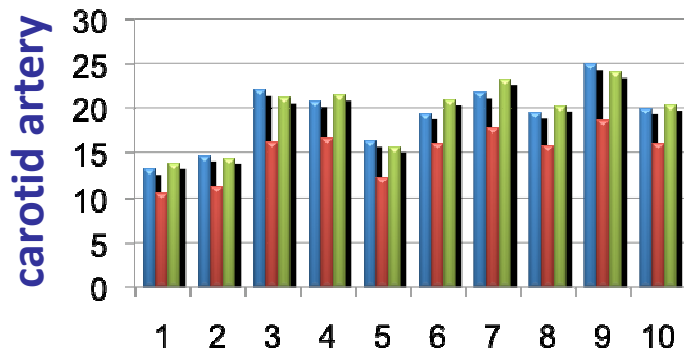
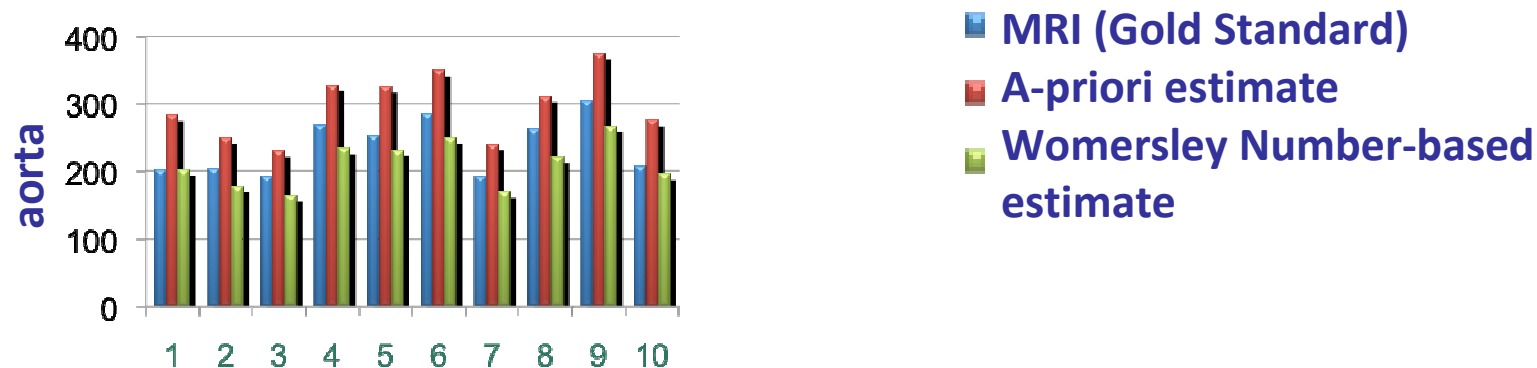
**Flow rate estimation**

**Error estimate**

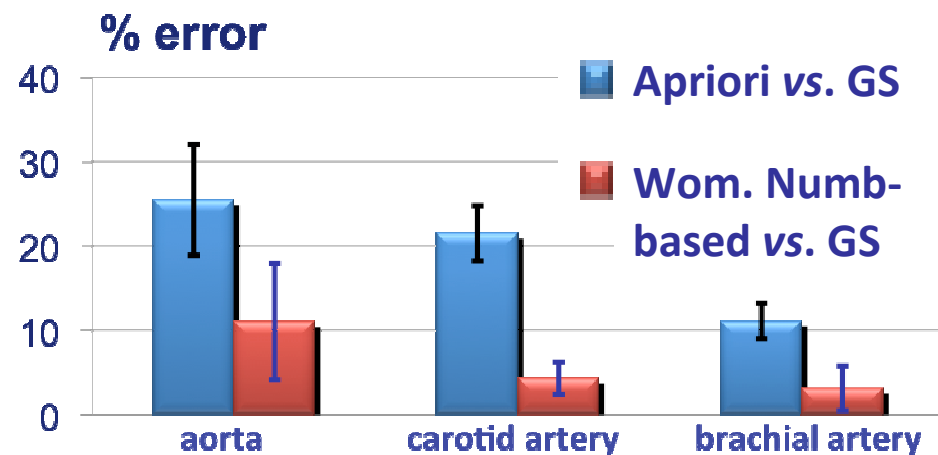


## Results: A-priori V.S. Womersley number-based estimates

### Flow rates calculations



- MRI (Gold Standard)
- A-priori estimate
- Womersley Number-based estimate

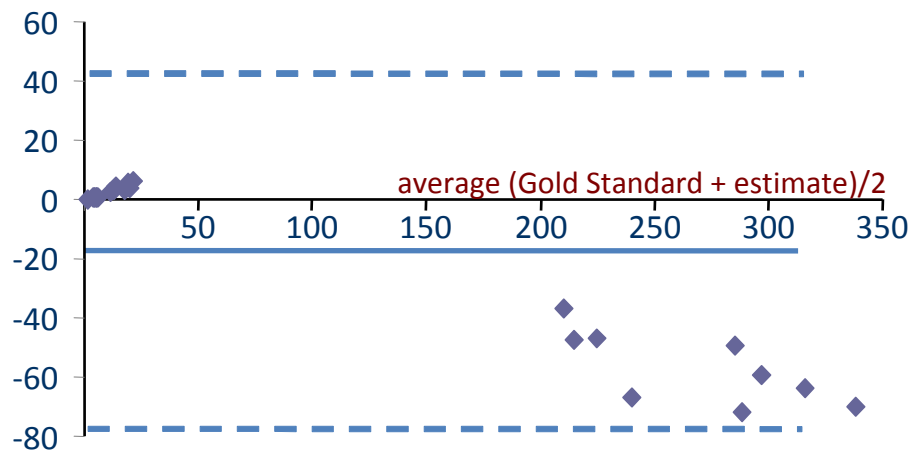




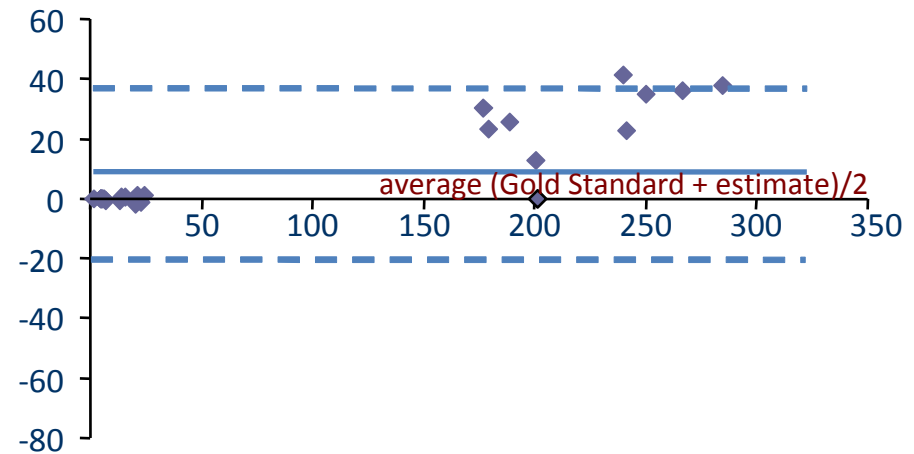
## Discussion: Bland-Altman confirmation

The Bland-Altman test confirms that the Womersley number-based approach is a more trustable estimate approach at the peak instant with the respect to the a-priori one

- ◆ MRI (Gold Standard) – estimate
- Average (GS – estimate)
- - - 2 stdv (GS-estimate)



A-priori formula

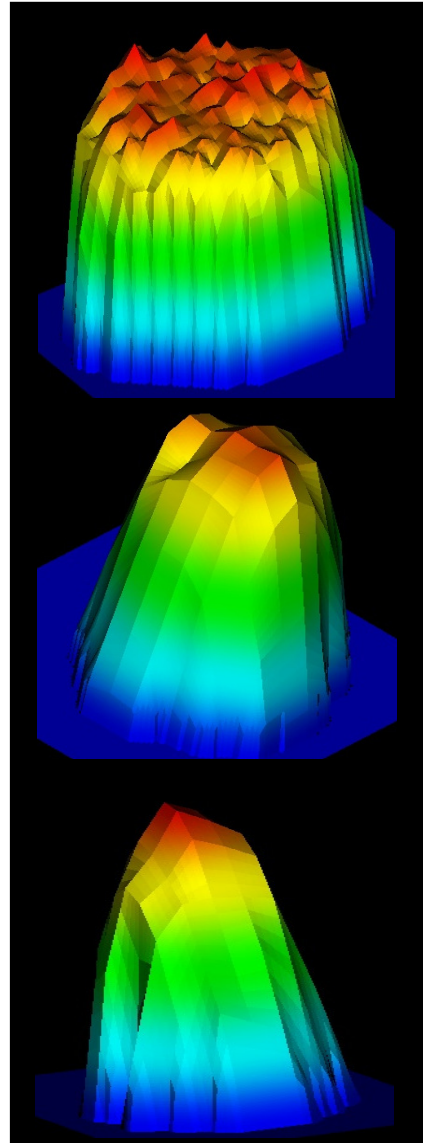


Womersley number-based formula



## *We can visualize the reason why in 3D*

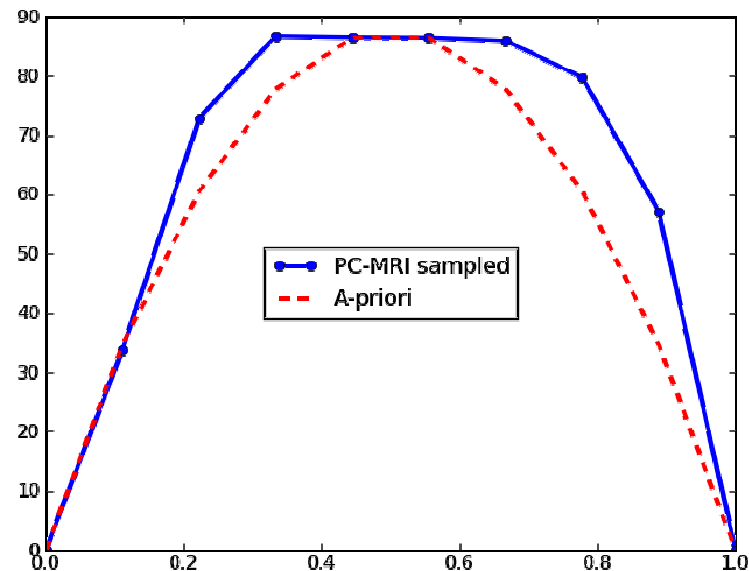
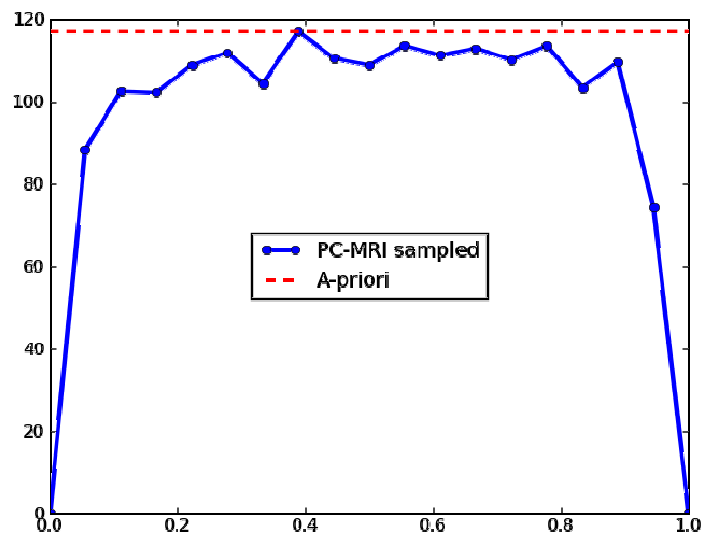
A cylindrical symmetry seems to be present



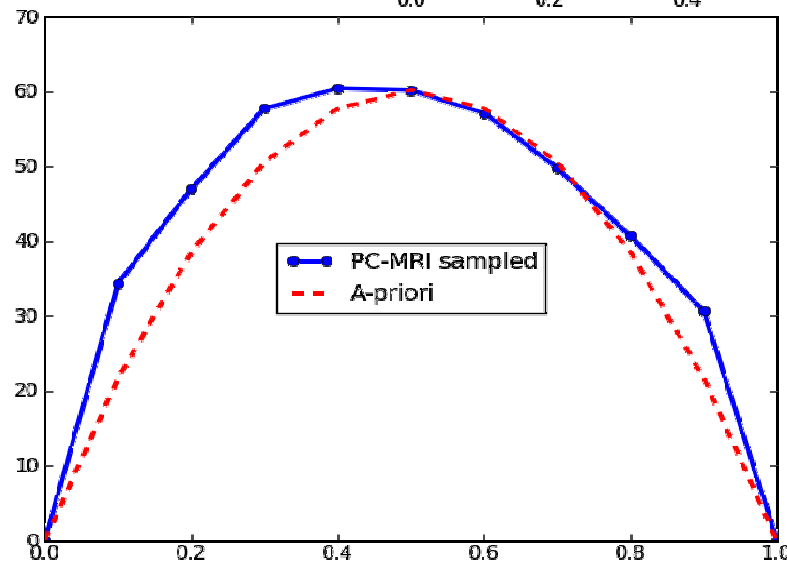
Nevertheless if we analyze more in depth the shape of the spatial velocity profile at the peak...



## We can visualize the reason why in 2D



... we found that a parabola or a flat profile are too rough approximation





## Conclusions

The results provided by this in vivo validation authorize us to state that:

1. The **Womersley number-based** new formula can give sensible more accurate blood flow rate estimates at the same practical cost of the **a-priori** formula thanks to its ability of take into account for blood pulsatility
2. The method is optimized at the moment to provide peak flow rate estimate
3. This approach is very general but can be tuned and adapted for any specific clinical case in order to obtain more accurate estimate (*eg curved vessels; occluded vessels, etc.*).



**USE THE WOMERSELY BASED  
APPROACH INSTEAD OF THE A-  
PRIORI CHOICE OF A VELOCITY  
PROFILE**



## *Medical devices CFD*

- Magnetic vascular positioner (MVP)
- Arterial line filters (ALF)
- Bileaflet prosthetic heart valve



## *Magnetic vascular positioner (MVP)*

Local fluid dynamics plays a central role on the onset/development of vessel's wall pathologies: **thrombogenesis, atherogenesis, endothelial damage, intimal thickening and hyperplasia.**

A still-debated relationship exists between peculiar blood flow patterns and physiopathological events (Moore et al, 1994; Karino and Goldsmith, 1984; Ku et al., 1985; Friedman et al., 1981): the detailed knowledge of local hemodynamics in realistic vessel geometries becomes topical.

At the moment several wall indexes (Wall Shear Stress-related) are used to quantify the occurrences of physiopathological events in human vessels. Among them:

$$\mathbf{TAWSS} = \frac{1}{T} \int_0^T |\mathbf{WSS}| \cdot dt$$

**T** is the heart period  
**WSS** is the Wall Shear Stress

$$\mathbf{OSI} = 0.5 \left[ 1 - \frac{\left| \int_0^T \mathbf{WSS} \cdot dt \right|}{\int_0^T |\mathbf{WSS}| \cdot dt} \right]$$



## *Helicity Index*

### Density of Kinetic Helicity

$$H_k(\mathbf{s}; t) = \mathbf{V} \cdot (\nabla \times \mathbf{V}) = \mathbf{V}(\mathbf{s}; t) \cdot \boldsymbol{\omega}(\mathbf{s}; t)$$

### Helicity

$$H(t) = \int H_k(\mathbf{s}; t) \, ds = \int \mathbf{V}(\mathbf{s}; t) \cdot \boldsymbol{\omega}(\mathbf{s}; t) \, ds,$$

where  $\boldsymbol{\omega} = \nabla \times \mathbf{V}$  is the vorticity field of the flow

### Normalized helicity index

$$\Psi(\mathbf{s}; t) = \frac{\mathbf{V}(\mathbf{s}; t) \cdot \boldsymbol{\omega}(\mathbf{s}; t)}{|\mathbf{V}(\mathbf{s}; t)| |\boldsymbol{\omega}(\mathbf{s}; t)|} \quad -1 \leq \Psi \leq 1$$



## Helical Flow Index

Using all the values of  $\Psi$ , computed along several particle trajectories, a quantitative determination of the helical blood flow inside a vessel can be done.

The mean quantity  $\Phi$  computed with this Lagrangian approach is the so called Helical Flow Index:

$$\Phi = \text{HFI} = \frac{1}{N_p} \sum_{k=1}^{N_p} \frac{1}{N_k} \sum_{j=1}^{N_k} |\Psi_{k,j}|_j \quad 0 \leq \Phi \leq 1$$

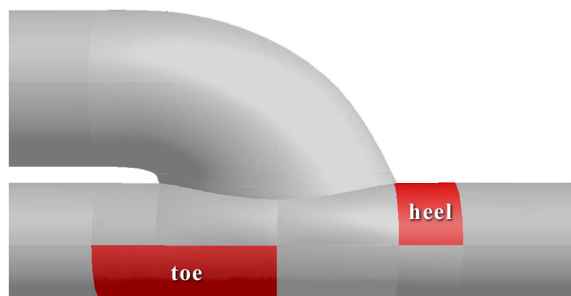
Where  $N_p$  is the number of particles and  $N_k$  is the number of points  $j$  ( $j=1, \dots, N_k$ ) in the  $k$ -th trajectory ( $K=1, \dots, N_p$ ) in which the index  $\psi$  is calculated



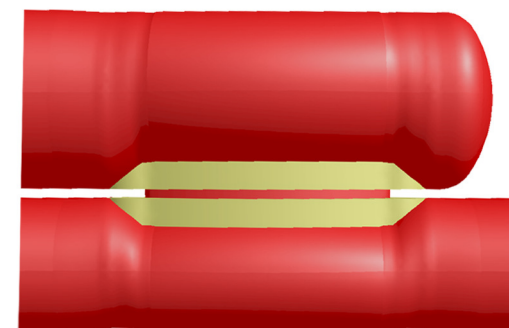
## Magnetic Vascular Positioner For Coronary Artery Bypass Grafting



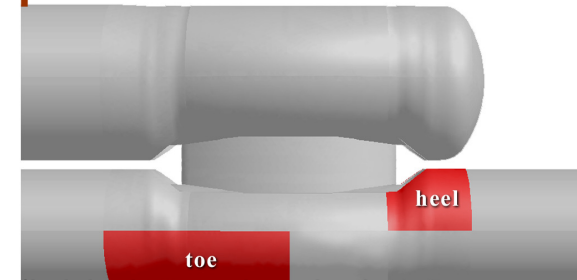
**Hand-sewn anostomosis**



The purpose of this application is to obtain a detailed comparison between the flow and WSS patterns in a distal hand-sewn anastomosis and the one performed with the magnetic vascular positioner (MVP)



**Magnetic vascular positioner anostomosis**



To evaluate the wall shear stress in the anastomotic region, three fluid dynamics indexes were used: the time average WSS value (TAWSS), the oscillatory shear stress index (OSI) and the helicity index  $\Psi$ . **The TAWSS and OSI indexes were calculated at the toe and heel regions of the models.**



## Geometrical features of the MVP model

All the geometrical features of the reconstructed model are based on optical microscopy analysis

A projection normal to the frontal view has been performed. Points A, B, C, D, E, F have been connected using circular arches.

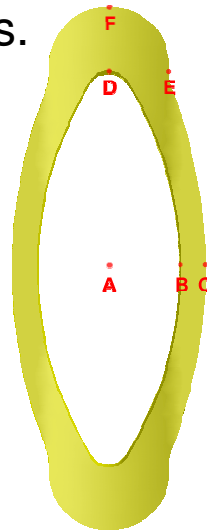
$$AB = 1 \text{ mm}$$

$$BC = 0.33 \text{ mm}$$

$$AD = 2.77 \text{ mm}$$

$$DF = 0.85 \text{ mm}$$

$$DE = 0.82 \text{ mm}$$

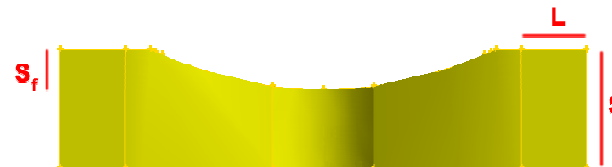


From the side view of the model the variation of the thickness of the reconstructed model can be appreciated.

$$L = 0.33 \text{ mm}$$

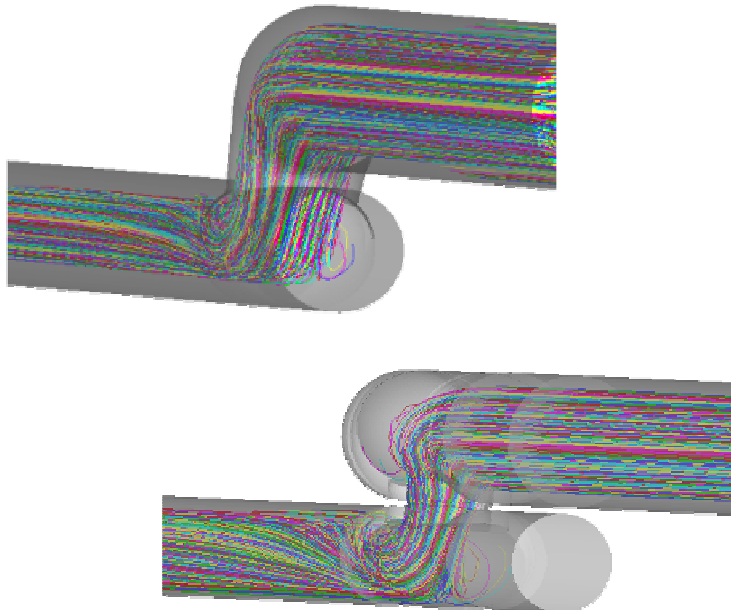
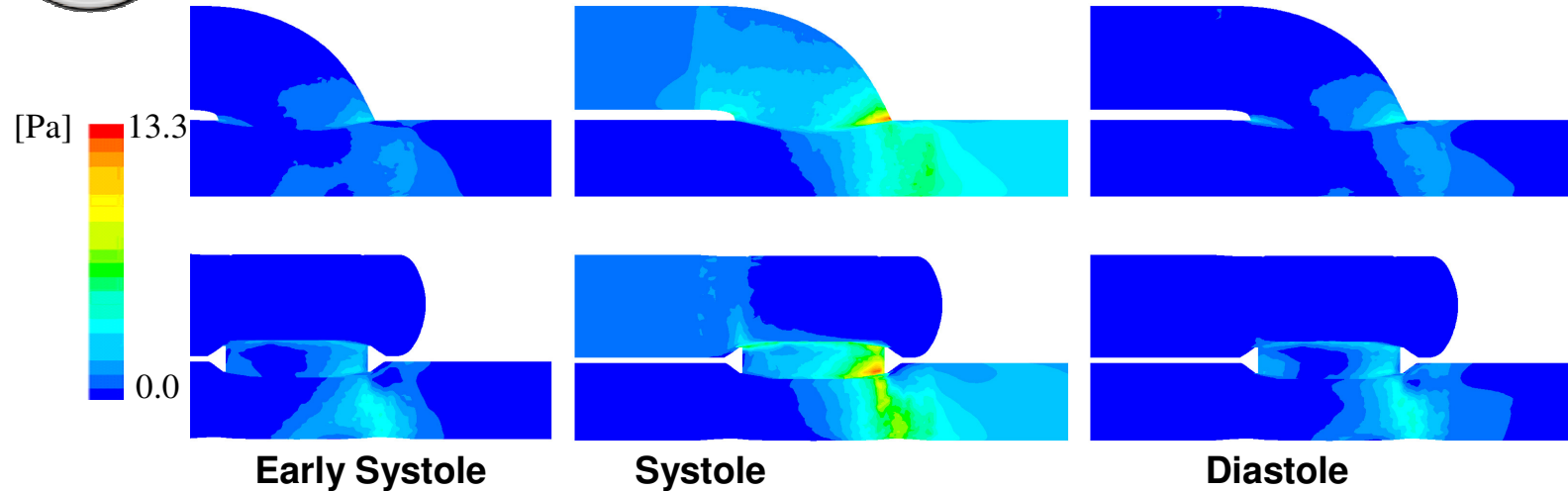
$$S = 0.6 \text{ mm}$$

$$S_f = 0.2 \text{ mm}$$





## Qualitative results



A set of emitters within the inlet surface of the graft was simulated for the release of  $N_p = 830$  massless particles that trace the temporal evolution of blood flow velocities over the entire cardiac cycle. A sensitivity study for  $\Psi$  and  $\Phi$  was also carried out, simulating the injection of the cluster of particles at four different phases  $T_n$  ( $n=1, \dots, 4$ ) of the cardiac cycle, and extracting their trajectories for the time duration  $T$  of one cycle (i.e.,  $T_n + T$ ).



## Quantitative results

Due to the vortex areas, in the two models, low and oscillating WSS were observed at the heel and toe regions, with very similar values with the MVP model.

Concerning the WSS for both models of the hand sewn anastomosis and the MVP, the maximum values were obtained at the diastolic peak and were located at the anterior wall of the anastomosis, with a magnitude of 13.3 Pa and 18.4 Pa, respectively.

The value of helical flow index reflect these observation and confirm that from a fluid dynamical point of view the two model shows the same characteristics

time of particles injection	Hand-sewn $\Phi$	MVP $\Phi$
$T_1$	0.272	0.243
$T_2$	0.268	0.237
$T_3$	0.260	0.237
$T_4$	0.249	0.227
$\Phi_{avg}$ (mean $\pm$ sd)	0.262 $\pm$ 0.010	0.236 $\pm$ 0.007



## ***Conclusion and perspectives : alternative quantitative index***

- ❑ Helical flow index **is directly related (linear inverse relationship) to OSI** and can furnish the same kind of knowledge.
- ❑ Helical flow index can become an **alternative quantitative index** with respect to wall indexes that require detailed knowledge of the WSS when this information is difficult to obtain or either very uncertain (Imaging segmentation problems).
- ❑ Helical flow index is able to catch important modifications of the flow patterns related to haemodynamics conditions (degree of stenosis).
- ❑ Helicity plays a significant role in the tuning of the cells' mechano-transduction pathways, highlighting the existence of a relationship between helical flow patterns and transport phenomena that could affect blood-vessel wall interaction.



## Arterial Line Filters (ALF)

ALF Prototype	AF6	AF8
Filtering screen surface area (cm <sup>2</sup> )	340.0	460.0
Inner volume (ml)	105.0	135.0
Max. rated blood flow (L/min)	6.0	8.0
CFD Discretization (million cells)	4.5	6.0

Using the same approach  
(Eulero/Lagrangian approach)

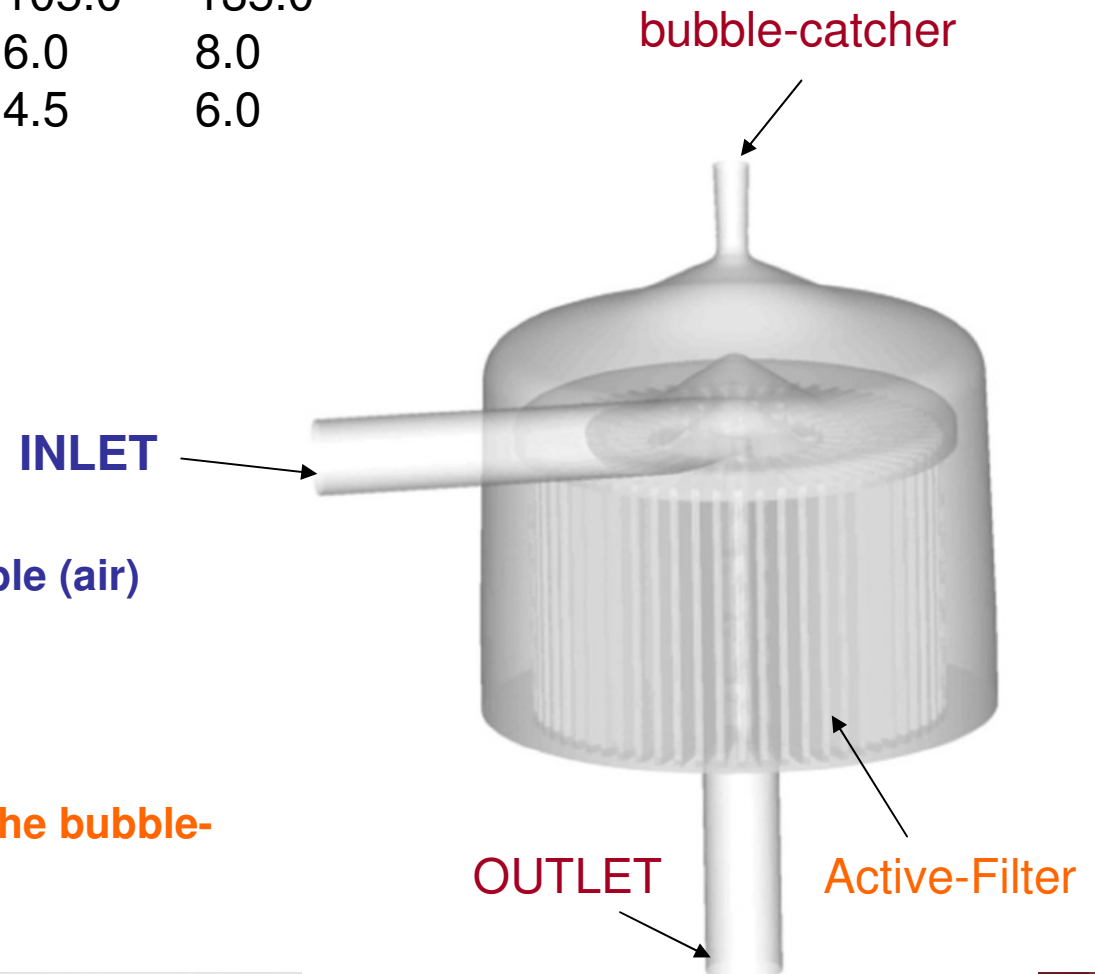
+

Different material properties of the bubble (air)

Different sizes of the bubbles

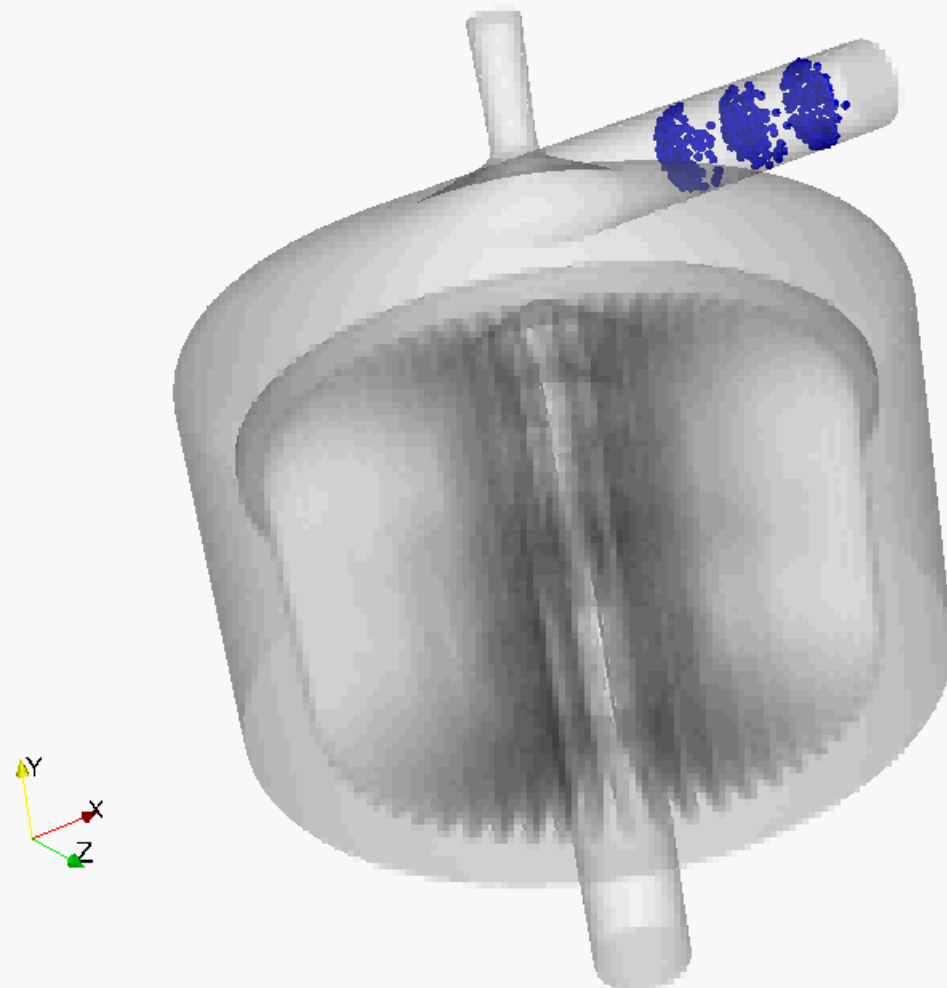
+

Trapping properties of the filter and of the bubble-catcher



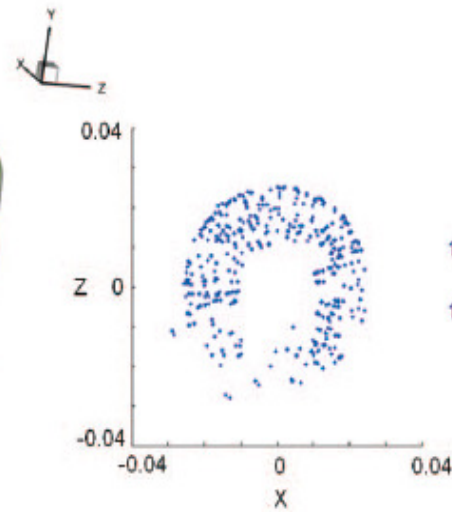


## Qualitative Results

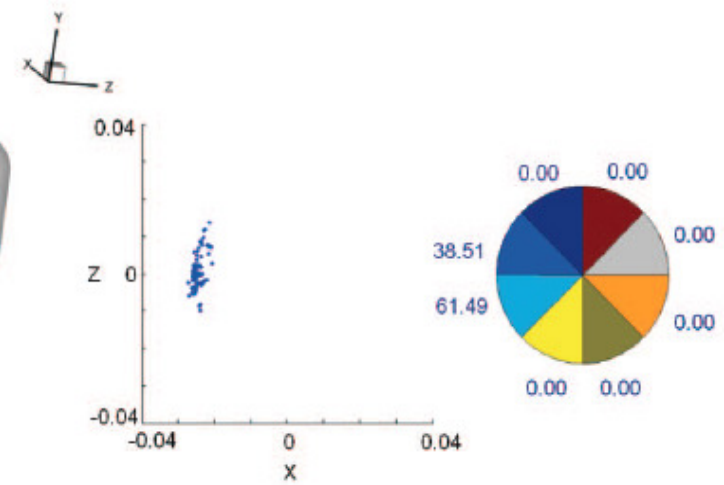




# Quantitative Results



30  $\mu\text{m}$  bubbles



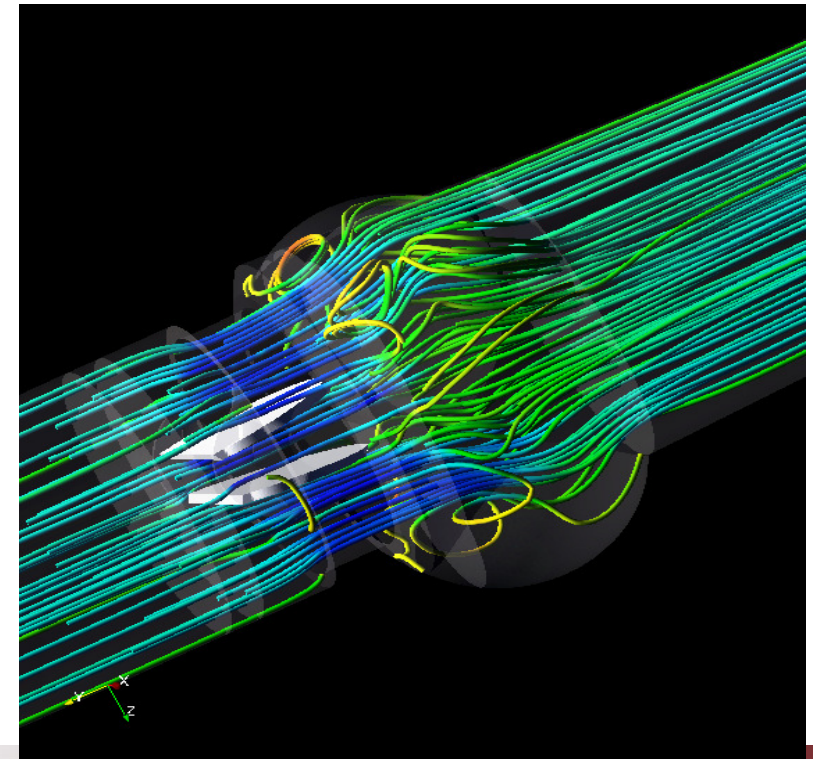
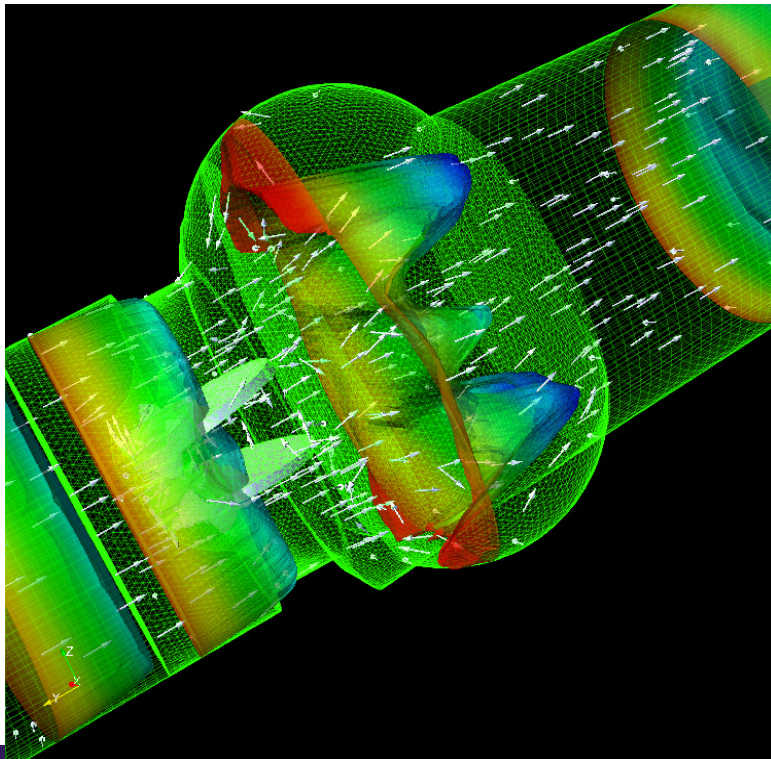
1000  $\mu\text{m}$  bubbles



## ***Bileaflet prosthetic heart valve***

Based on the work of the **PhD. Thesis of Matteo Nobili** (Enginsoft) developed at Politecnico di Milano (Dept. of Bioengineering) we studied FSI for a bileaflet hearth valve

- ❑ Particle data calculation using the same paradigm discussed above:  
Platelet activation
- ❑ Feasibility study of DNS simulation: a comment





## ***Platelet activation***

Risk of cardioembolic stroke is the major impediment to implantable blood recirculating devices

### Mechanical Heart Valves —Flow Induced Emboli Formation

chronic platelet activation and the initiation of thrombus formation is the salient aspect of flow induced blood trauma in MHV

flow phases characterized by elevated stresses (shear, deformation, and turbulent)

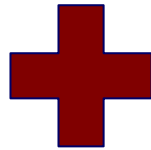
platelet activation by flow stresses may occur at any of the phases

free emboli formed in the wake of the valve during the forward flow phase, enhance the risk of systemic emboli



## Overall approach

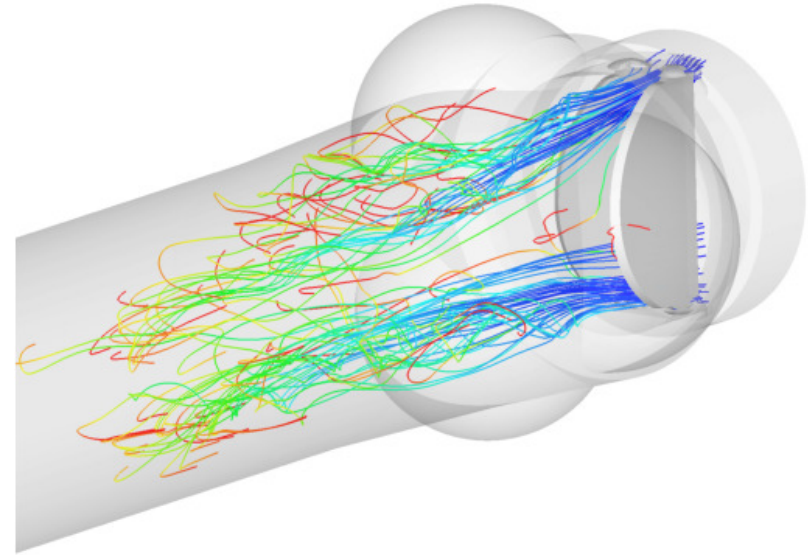
Depiction of the flow fields  
through the MHV  
*in silico* FSI approach



Prediction of the flow-induced  
platelet activation level  
Lagrangian based mathematical  
model  
shear-induced blood trauma

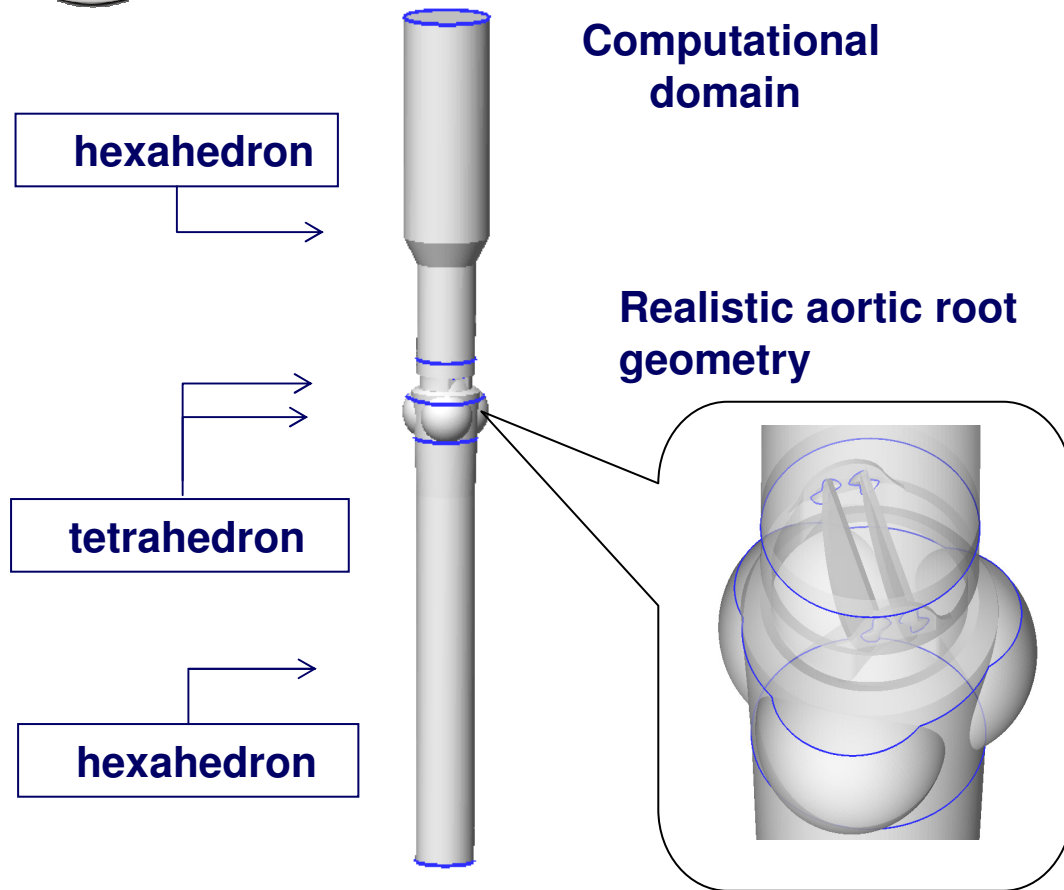


Evaluation of the thrombogenic  
potential of the valve





# MHV FSI SIMULATIONS



## St. Jude Hemodynamic Plus



**Flow rate** = 4.5 l/min

**Re<sub>mean</sub>** = 3775

**Blood flow:** incompressible,  
Newtonian fluid (3.7 cP);

**Time-step:** 2.10<sup>-4</sup> s.



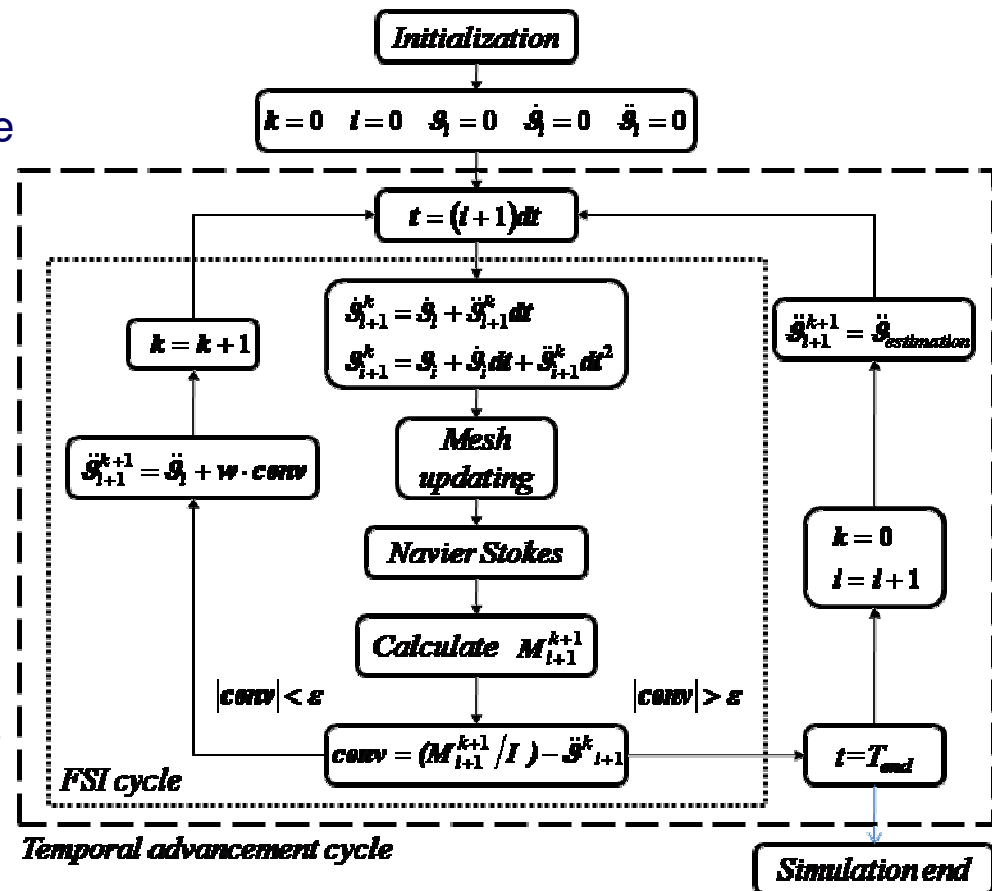
# MHV FSI SIMULATIONS

Implicit coupling procedure scheme of the interaction between the valve leaflet and the blood flow:

- $\theta$  angular position of the leaflet the position;
- $i$  time step number;
- $k$  number of FSI iteration within the same time step;
- $\omega$  = under relaxation coefficient;
- $\varepsilon$  = FSI convergence threshold.

Two loops are annealed:

- the loop which checks for the convergence of the FSI procedure (inner loop);
- the temporal advancement loop which makes the simulation proceeds to the next time step starting from the acceleration of the leaflet calculated at the end of the previous one





## MHV FSI SIMULATIONS

Implicit coupling procedure scheme of the interaction between the valve leaflet and the blood flow

*fluid dynamics simulation*

**valve acceleration**



$$I\ddot{\vartheta}_{i+1} = Mp_{i+1} + M\tau_{i+1}$$



**moment acting on the valve**

*valve motion calculation*



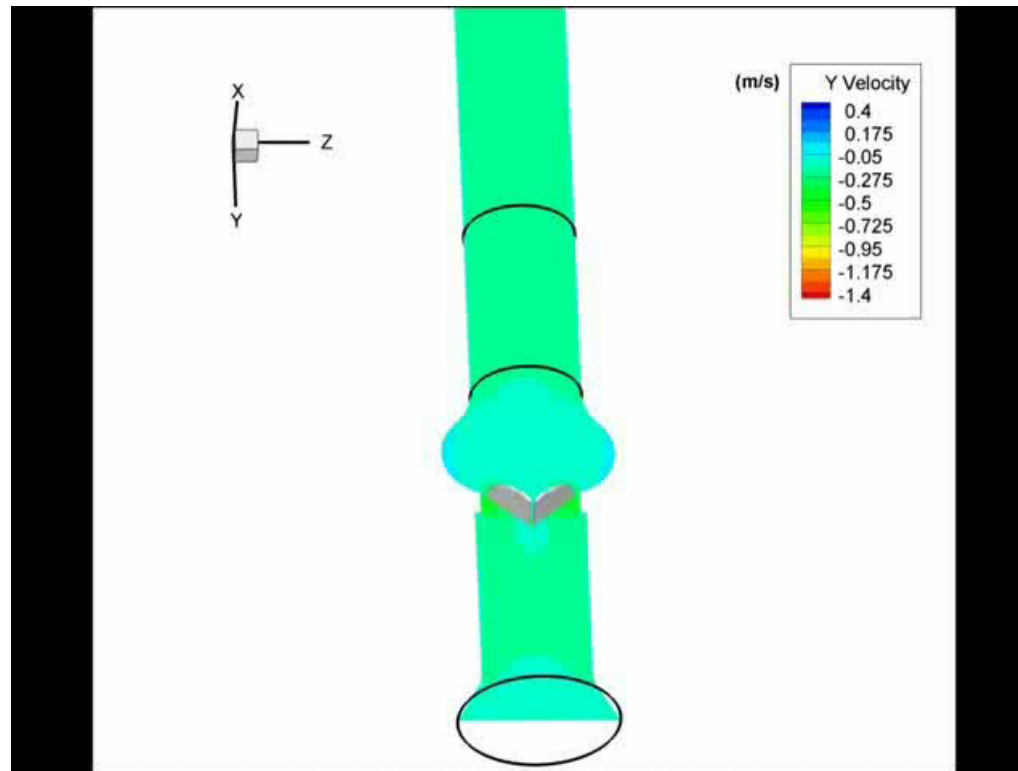
## ***MHV FSI SIMULATIONS - VALIDATION***

To validate the numeric prediction of the dynamics of the leaflets, we compared the computed leaflets displacement with experimental data (Redaelli et al., 2004; Nobili et al., 2008). Experimental study performed using ultrafast cinematographic technique during the working cycle of the MHV in the Vivitro System mock loop.

Redaelli A., Bothorel H., Votta E., Soncini M., Morbiducci U., Del Gaudio C., Balducci A., Grigioni M., 2004. 3-D simulation of the SJM bileaflet valve opening process: fluid-structure interaction study and experimental validation. *Journal of Heart Valve Disease*; 13:804-813.

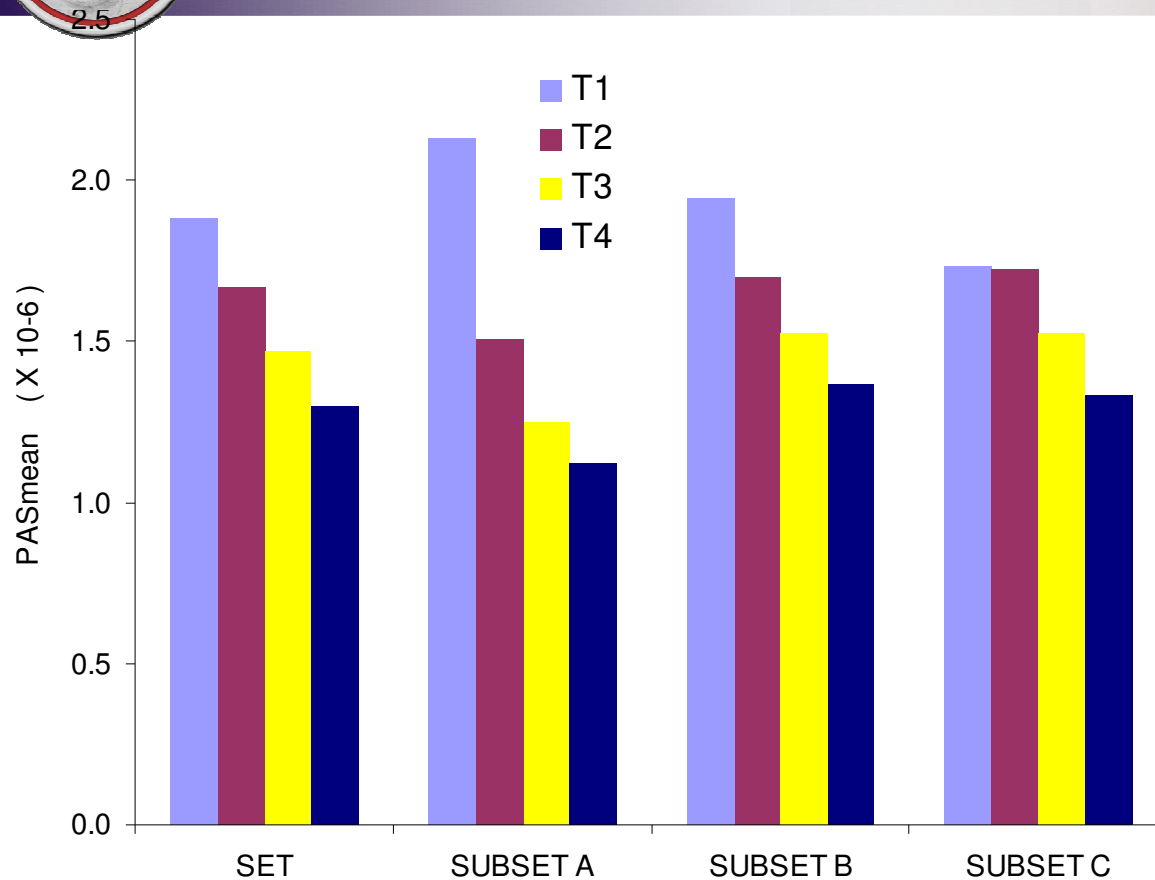


## Qualitative results





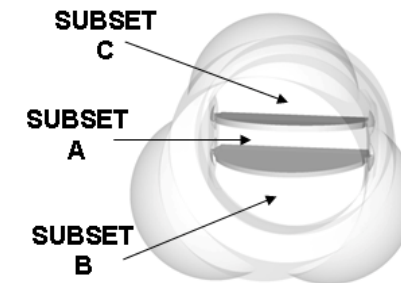
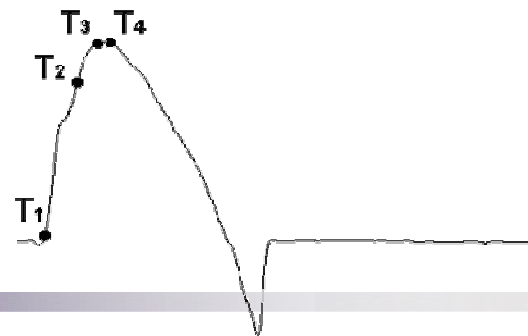
## Quantitative Results: Platelet Activation



Platelets passing through the central orifice (subset A) are characterized by PAS values:

i) higher than subsets B, C when emitted at early systole ( $T_1$ );

ii) lower than subsets B and C when emitted at  $T_2 - T_4$





## ***Conclusions***

We have applied FSI modeling, incorporating a robust model for quantifying the cardioembolic potential of MHVs.

The proposed “comprehensive scale” approach:

- ❑ allows a comparison of the platelets activation state reached at various time instants while flowing through the valve
- ❑ accounts for differences in exposure time among platelets during the various flow phases of the cardiac cycle, and adjusts the model predictions accordingly
- ❑ great potential for benchmark studies, because a wide variety of flow conditions, valve orientations, design features can be modeled computationally, and the results can be easily compared
- ❑ could provide an efficient assessment tool for MHV performance and possibly lead to improved valve designs



## *now...looking for the DNS*

Reynolds number value equal to 6000, and a mean Reynolds number value equal to 3775. Hence, the Kolmogorov scale of the investigated flow field results in the order of 0.04 and 0.06mm for the maximum and the mean Reynolds respectively

### *Preliminary study of feasibility on HPC environment*

From the 2.1 million of cells model (about 0.6 mm, up to Taylor scale), using a grid-adaption algorithm we built:

$2 \times 8 = 16$  million cells model



## *Application of CFD algorithms to human flow data*

- Scientific visualization in vivo
- 7D FlowViz



## ***Scientific visualization in vivo***

Visualize in vivo data by means of CFD algorithms and approach is now feasible thanks to IMAGING TECHNIQUES such as Phase Contrast MRI.

The 4D nature of the tri-directional velocity components (7D complexity) of the blood flow field is now acquirable with this non-invasive technique.

The reliability of in-vivo data processing is still doubtful due to low spatial/temporal accuracy.

CFD can be used again as a privileged yet simple and realistic experimental environment to test to which extent these kind of innovative processing is feasible and accurate.

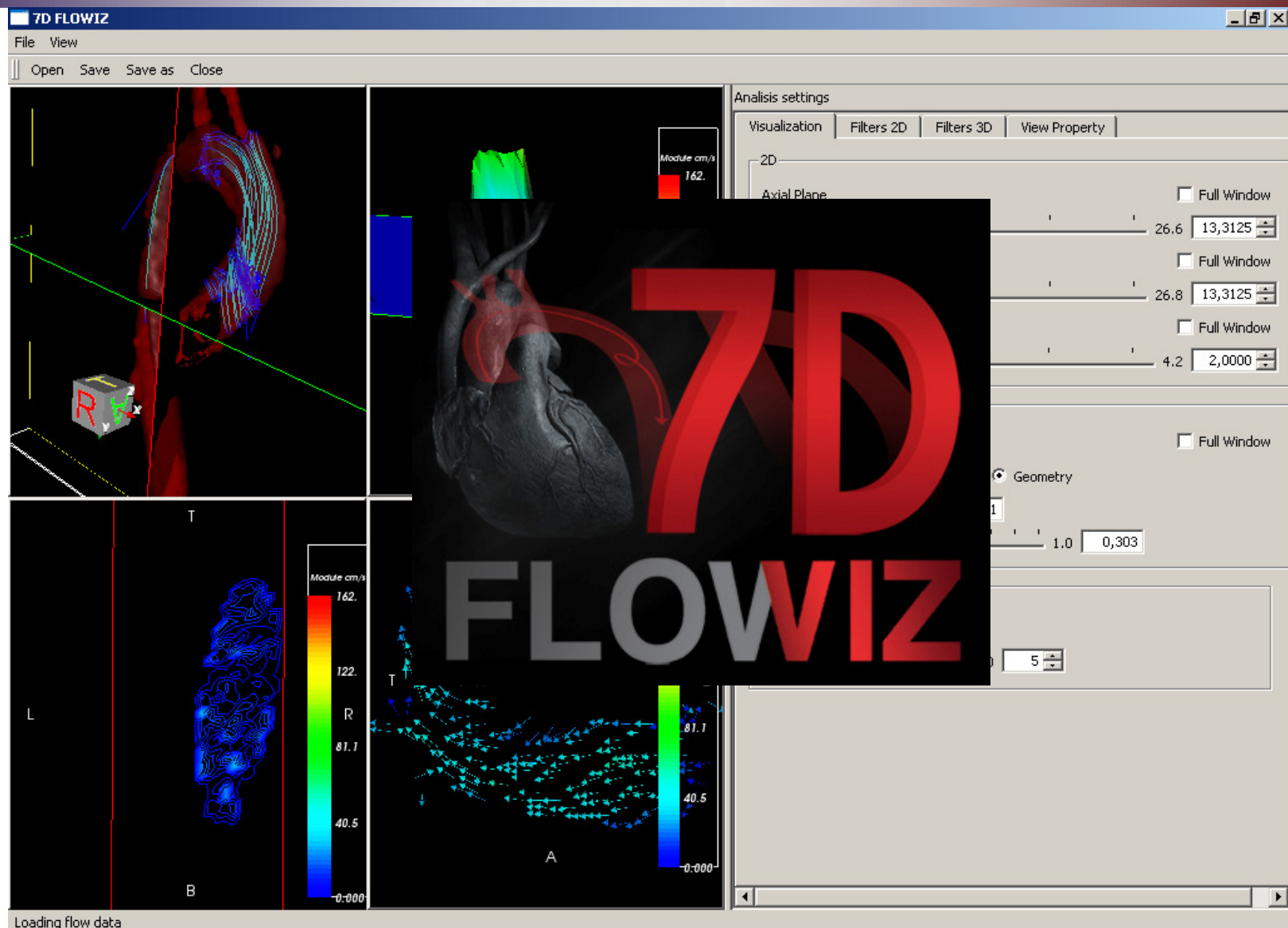
*“In vivo calculations of haemodynamic descriptors using cine PC MRI. Algorithms evaluation by means of tailored CFD-based 4D dataset generation.”*

*Raffaele Ponzini, PhD.; Umberto Morbiducci, PhD.; Giovanna Rizzo, Eng.; Francesco Iannaccone, Eng.; Alberto Redaelli, Prof.*

*Submitted to Medical Engineering & Physics*



## From CFD to in vivo calculation: 7D FloWviz





## References

- ❑ Vergara, C., Ponzini, R., Veneziani, A., Redaelli, A., Neglia, D., & Parodi, O. (2009). Womersley number-based estimation of flow rate with doppler ultrasound: Sensitivity analysis and first clinical application. *Computer Methods and Programs in Biomedicine*
- ❑ Fiore, G. B., Morbiducci, U., Ponzini, R., & Redaelli, A. (2009). Bubble tracking through computational fluid dynamics in arterial line filters for cardiopulmonary bypass. *ASAIO Journal*, 55(5), 438-444.
- ❑ Morbiducci, U., Ponzini, R., Nobili, M., Massai, D., Montevvecchi, F. M., Bluestein, D., et al. (2009). Blood damage safety of prosthetic heart valves. shear-induced platelet activation and local flow dynamics: A fluid-structure interaction approach. *Journal of Biomechanics*, 42(12), 1952-1960.
- ❑ Ponzini, R., Rizzo, G., Vergara, C., Veneziani, A., Morbiducci, U., Montevvecchi, F. M., et al. (2009). Computational modeling of local hemodynamics phenomena: Methods, tools and clinical applications. *Nuovo Cimento Della Societa Italiana Di Fisica C*, 32(2), 77-80.



## References

- ❑ Morbiducci, U., Ponzini, R., Rizzo, G., Cadioli, M., Esposito, A., De Cobelli, F., et al. (2009). In vivo quantification of helical blood flow in human aorta by time-resolved three-dimensional cine phase contrast magnetic resonance imaging. *Annals of Biomedical Engineering*, 37(3), 516-531.
- ❑ Ponzini, R., Lemma, M., Morbiducci, U., Montevecchi, F. M., & Redaelli, A. (2008). Doppler derived quantitative flow estimate in coronary artery bypass graft: A computational multiscale model for the evaluation of the current clinical procedure. *Medical Engineering and Physics*, 30(7), 809-816.
- ❑ Nobili, M., Morbiducci, U., Ponzini, R., Del Gaudio, C., Balducci, A., Grigioni, M., et al. (2008). Numerical simulation of the dynamics of a bileaflet prosthetic heart valve using a fluid-structure interaction approach. *Journal of Biomechanics*, 41(11), 2539-2550.
- ❑ Morbiducci, U., Lemma, M., Ponzini, R., Boi, A., Bondavalli, L., Antona, C., et al. (2007). Does the ventricle magnetic vascular positioner (MVP®) for coronary artery bypass grafting significantly alter local fluid dynamics? A numeric study. *International Journal of Artificial Organs*, 30(7), 628-639.



## *References*

- ❑ Morbiducci, U., Ponzini, R., Grigioni, M., & Redaelli, A. (2007). Helical flow as fluid dynamic signature for atherogenesis risk in aortocoronary bypass. A numeric study. *Journal of Biomechanics*, 40(3), 519-534.
- ❑ Ponzini, R., Vergara, C., Redaelli, A., & Veneziani, A. (2006). Reliable CFD-based estimation of flow rate in haemodynamics measures. *Ultrasound in Medicine and Biology*, 32(10), 1545-1555.

# THANK YOU